ELSEVIER

Nuclear Instruments and Methods in Physics Research B 192 (2002) 117–127

NIM B
Beam Interactions with Materials & Atoms

www.elsevier.com/locate/nimb

Sympathetically laser-cooled positrons ☆

B.M. Jelenković [a,b], A.S. Newbury [a,c], J.J. Bollinger [a,*], T.B. Mitchell [a,d], W.M. Itano [a]

[a] Time and Frequency Division, National Institute of Standards and Technology, 325 Broadway, Boulder, CO 80305, USA
[b] Institute of Physics, University of Belgrade, Pregrevica 118, 11080 Zemun, Belgrade, Yugoslavia
[c] Ball Aerospace, Boulder, CO 80301, USA
[d] Department of Physics and Astronomy, University of Delaware, Newark, DE 19716, USA

Abstract

We present results on trapping and cooling of positrons in a Penning trap. Positrons from a 2 mCi ^{22}Na source travel along the axis of a 6 T magnet and through the trap after which they strike a Cu reflection moderator crystal. Up to a few thousand positrons are trapped and lose energy through Coulomb collisions (sympathetic cooling) with laser-cooled $^{9}Be^{+}$. By imaging the $^{9}Be^{+}$ laser-induced fluorescence, we observe centrifugal separation of the $^{9}Be^{+}$ ions and positrons, with the positrons coalescing into a column along the trap axis. This indicates the positrons have the same rotation frequency and comparable density ($\sim 4 \times 10^{9}$ cm^{-3}) as the $^{9}Be^{+}$ ions, and places an upper limit of approximately 5 K on the positron temperature of motion parallel to the magnetic field. We estimate the number of trapped positrons from the volume of this column and from the annihilation radiation when the positrons are ejected from the trap. The measured positron lifetime is >8 days in our room-temperature vacuum of 10^{-8} Pa. Published by Elsevier Science B.V.

1. Introduction

This paper presents experimental results on the capture, storage and cooling of positrons in a Penning trap that simultaneously contains laser-cooled $^{9}Be^{+}$ ions. The experimental work follows previous discussions and simulations of trapping and sympathetic cooling of positrons via Coulomb collisions with cold $^{9}Be^{+}$ ions [1,2]. Cold positron plasmas are useful as a source for cold beams of high brightness [3–6]. In addition cold positron plasmas are useful for studies of positron–normal-matter interactions, such as the study of resonances in low-energy positron annihilation on molecules [3], for production of a plasma whose modes must be treated quantum mechanically [1,7,8], and for formation of antihydrogen by passing cold antiprotons through a reservoir of cold positrons [9–11].

Several groups have successfully trapped positrons in electromagnetic traps. Positrons have been trapped using resistive cooling of the positrons [12], by ramping the trap electrostatic potential [13] and in a magnetic-mirror configuration by electron cyclotron resonance heating [14]. Recent experiments by Gabrielse and co-workers [15–17] have successfully trapped more than 10^{6} positrons in 17 h through a method where apparently

☆ Contribution of the National Institute of Standards and Technology. Not subject to US copyright.

* Corresponding author.
E-mail address: jjb@boulder.nist.gov (J.J. Bollinger).

0168-583X/02/$ - see front matter Published by Elsevier Science B.V.
PII: S0168-583X(02)00791-7

positronium in a high Rydberg state created on the surface of the moderator is field-ionized in the trap. They used a 3 mCi positron source and a tungsten positron moderator in the experiment. The positrons were cooled by thermalization with a cryogenic Penning trap which ensured a temperature of ~4 K. Surko and co-workers [3,5, 18–20], using a 90 mCi positron source, report the largest number of trapped positrons ($\sim 3 \times 10^8$) with a trapping rate of 3×10^8 positrons in 8 min and a trapping efficiency greater than 25% of the moderated positrons. The positrons were thermalized to room temperature since the trapping was achieved through collisions with a room-temperature buffer gas of N_2.

In this paper we will discuss the results of simultaneously trapping and cooling positrons with laser-cooled $^9Be^+$ ions. We observe centrifugal separation of the positrons and $^9Be^+$ ions, which enables us to determine the positron density and place a rough upper bound on the positron temperature. In Section 2 we describe the experiment, and in Section 3, the positron detection methods. In Section 4 we present the measured accumulation rates and positron lifetime. The discussion of our method for estimating temperature limits is presented in Section 5. We conclude by summarizing and discussing future possibilities.

2. Experimental setup

The Penning trap, along with the positron source and positron moderator are shown in Fig. 1. The stack of cylindrical electrodes (10 mm in diameter, 60 mm long) forms two Penning traps, enclosed in a quartz cylinder and placed parallel to the 6 T magnetic field. The top (load) trap was used to create $^9Be^+$ plasmas by ionizing neutral Be atoms sublimated from a heated Be filament and directed through a small hole on the ring electrode. The $^9Be^+$ ions are transferred to the lower (experimental) trap for experimentation. In a single load-transfer cycle we can store over one million ions. An axisymmetric, nearly quadratic trapping potential is generated by biasing the ring of the experimental trap to a negative voltage V_R and adjacent compensation electrodes to $V_C = 0.9 \times V_R$. For $V_R = -100$ V and for the endcap voltage $V_{EC} = 0$ the single particle axial frequency for $^9Be^+$ ions is $\omega_z = 2\pi \times 870$ kHz and the magnetron frequency is $\omega_m = 2\pi \times 35$ kHz.

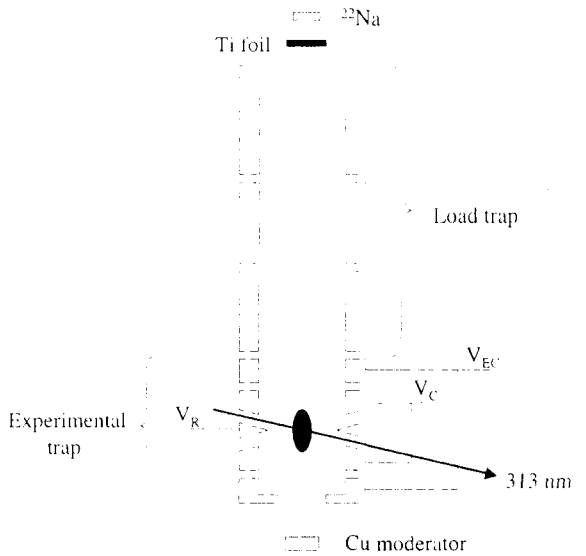

Fig. 1. Schematic diagram of the cylindrical Penning traps showing the load trap used to load $^9Be^+$ ions and experimental trap for experimentation with positrons and ions. V_R, V_C and V_{EC} are respectively the voltages applied to the ring, compensation and end cap electrodes of the experimental trap. The laser light at ~313 nm is directed through the ion plasma which is located at the center of the experimental trap.

The ions were cooled by a laser beam tuned ~10 MHz lower than a hyperfine-Zeeman component of the $2s^2S_{1/2} \rightarrow 2p^2P_{3/2}$ resonance at 313 nm. The laser beam was directed through the trap, intersecting the ion plasma on the side receding from the laser beam due to the plasma rotation. As shown in Fig. 1 the beam entered the trap between the upper compensation and ring electrodes, passed through the trap center, and exited through the gap between the ring and lower compensation electrode, making an 11° angle with the horizontal (x–y) plane. Based on measurements performed in previous experiments [21–23] we expect $T_\perp \leqslant T_\parallel \leqslant$ 100 mK, where $T_\perp$ and $T_\parallel$ describe the velocity distributions in the direction perpendicular and parallel to the trap axis (z axis).

An ion plasma in thermal equilibrium at these cryogenic temperatures is a uniform-density plasma with a rigid-body rotation frequency ω_r in

the range $\omega_m < \omega_r < \Omega - \omega_m$. The ion density is constant within the plasma and is given by $n_0 = 2\epsilon_0 m\omega_r(\Omega - \omega_r)/q^2$, where q and m are the charge and mass of an ion, and ϵ_0 is the permittivity of the vacuum. With the quadratic trapping potential near trap center, the plasma has the shape of a spheroid whose aspect ratio, $\alpha = z_0/r_0$, depends on ω_r. Here $2z_0$ and $2r_0$ are the axial and radial extents of the plasma spheroid. Low rotation ($\omega_r \sim \omega_m$) results in an oblate spheroid of large radius. Increasing ω_r increases the Lorentz force due to the plasma rotation through the magnetic field, which in turn increases α and n_0. At $\omega_r = \Omega/2$ (Brillouin limit) the ion plasma attains its maximum aspect ratio and density. For $^9Be^+$ ions at 6 T the maximum ion density is 1.1×10^{10} cm^{-3}. High density can be reached by using torques produced by a cooling laser beam [24] or by a rotating electric field perturbation [25,26] to control the plasma's angular momentum. Typically, the ions were first Doppler laser-cooled and ω_r was approximately set by the laser torque. The "rotating wall" was then turned on at a frequency near the rotation frequency of the $^9Be^+$ plasma. Resonantly scattered 313 nm photons were collected by an $f/5$ imaging system in a direction 11° above the $z = 0$ plane of the trap and imaged onto the photocathode of a photon-counting imaging detector. Such an optical system produces an approximate side-view image of the $^9Be^+$ plasma.

The source for the positrons was a 2 mCi ^{22}Na source with an active diameter of ~1 mm. The source is placed just above the vacuum envelope, and positrons enter the trap through a Ti foil of 7 μm thickness. Positrons travel along the axis of the Penning traps until they hit the moderator crystal placed below the lower end-cap of the experimental Penning trap. The positron current reaching the crystal was measured by an electrometer. At the beginning of our experiment the measured current was ~2 pA, in accordance with the expected positron losses in the Ti foil and the fringing fields of the magnet at the position of the ^{22}Na source. A thin chopper wheel was placed between the ^{22}Na source and the Ti foil for lock-in detection of the positron current (if needed) and to temporarily block the positrons from entering the trap without removing the ^{22}Na source.

For the method of trapping positrons discussed in [2], a room-temperature kinetic-energy distribution of moderated positrons is important. Room-temperature distributions of moderated positrons have been reported in the literature for a number of single-crystal metallic moderators. We chose a Cu(1 1 1) moderator crystal because of the expected narrow distribution of positrons [27,28], and because it can be annealed and cleaned at a lower temperature (~900 °C). The experimental results discussed here were obtained with the moderator crystal heated to 350 °C during the vacuum bakeout.

3. Positron detection

In the experiment, the presence of trapped positrons was verified by three different methods. The positrons were detected by our (a) observing changes in the $^9Be^+$ ion fluorescence due to application of the microwaves near the positron cyclotron frequency, (b) detecting the absence of $^9Be^+$ ions in the plasma center in side-view images of the $^9Be^+$ ion fluorescence and (c) detecting the annihilation radiation after pulsing the accumulated positrons onto the titanium foil (same foil that is at the top of the vacuum envelope). Fig. 2 is a schematic diagram of the different detection techniques.

3.1. Positron cyclotron excitation

The first evidence of positron trapping was obtained through microwave excitation of the positron cyclotron resonance near 166 GHz. Wave guides carry the microwave radiation into the magnet bore close to the trap center. The microwaves heated the positrons by increasing their cyclotron energy. Through the Coulomb interaction the positrons then increased the $^9Be^+$ ion energy, which changed the level of the $^9Be^+$ ion resonance fluorescence. The positron cyclotron resonance curve, obtained by sweeping the microwave radiation around 166 GHz, was ~200 kHz wide [29]. We believe the resonance width was probably caused by power broadening. Significant positron excitation appeared to be required to

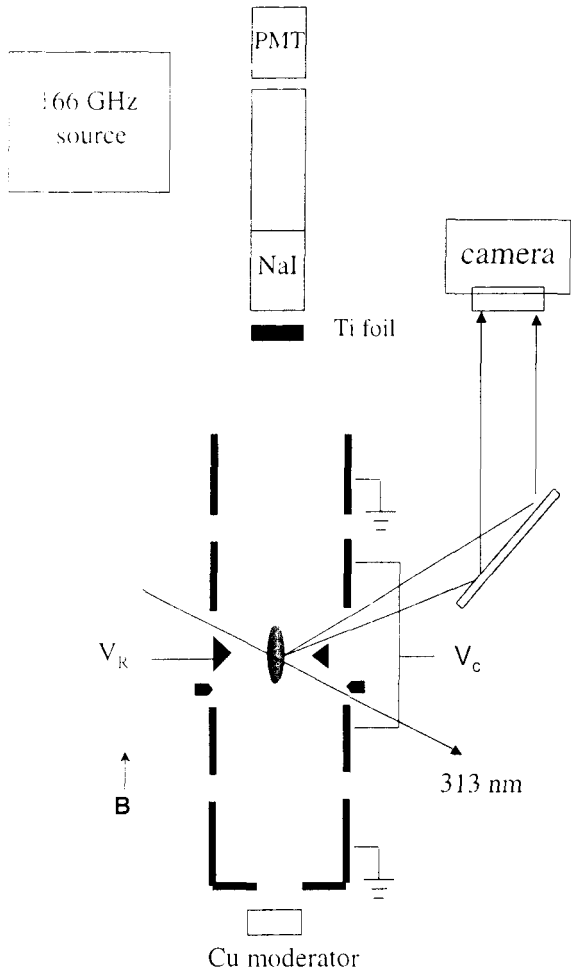

Fig. 2. Schematic diagram of the experimental Penning trap and the three techniques used for detecting positrons: e^+ cyclotron excitation with a 166 GHz source, e^+–$^9Be^+$ side-view images using $f/5$ optics and a camera, and a NaI scintillator with a photomultiplier tube.

observe the resonance because of the weak coupling between the positron cyclotron and $^9Be^+$ ion motions and the low rate of energy transfer between the positron cyclotron and axial energies in the high magnetic field of our trap [30]. Other potential sources of broadening include the relativistic mass shift (~10 kHz for each 300 K in energy), first-order Doppler broadening from positron motion within the trap, and magnetic field instability and inhomogeneity.

3.2. Centrifugal separation

Due to the plasma rotation, ion species with different charge-to-mass ratios tend to centrifugally separate in a Penning trap [31,32]. If ions with different q/m rotate about the trap axis at the same radius, they will tend to rotate with different rates because of different centrifugal forces. Collisional drag will cause a radial drift of the lighter ions inward, and the heavier ions outward, if the ions have the same charge. The different species will separate and the whole plasma will come to thermal equilibrium and rotate at uniform ω_r as a rigid body [32]. At low temperatures the density inside either species is constant, and drops to zero at the species boundaries within a distance on the order of the temperature-dependent Debye length. Therefore, trapped positrons, if cooled, will move to smaller radii than the $^9Be^+$ ions. In the limit of zero temperature, the edges of each plasma will be sharp (Debye length $\rightarrow 0$), and the plasmas will completely separate, with the positrons forming a column of uniform density along the trap axis. If the $^9Be^+$ plasma density is significantly below the Brillouin limit, the e^+ and $^9Be^+$ densities are expected to be approximately equal and the plasma separation quite small [7,32].

Fig. 3 shows an image of a $^9Be^+$–e^+ plasma along with the radial dependence of the fluorescence signal. The $^9Be^+$ ion density n_0 is calculated from the rotation frequency ω_r set by the rotating wall. With approximately equal density for both species, the number of positrons in the "dark" column of the plasma image is $n_0 \times V$, where V is the volume of the "dark" region.

If any ions with a charge-to-mass ratio greater than $^9Be^+$ are created during the positron accumulation, they will also centrifugally separate and contribute to the size of the non-fluorescing column in the plasma center. With the ^{22}Na source blocked, we deliberately created singly charged light-mass ions by ionizing background gas with a ~15 eV electron beam. From the volume of the central dark region as a function of time, the lifetime of the light-mass ions was measured to be less than 10 h. Similar measurements were performed after accumulating positrons and are discussed in more detail in the next section. In this case very

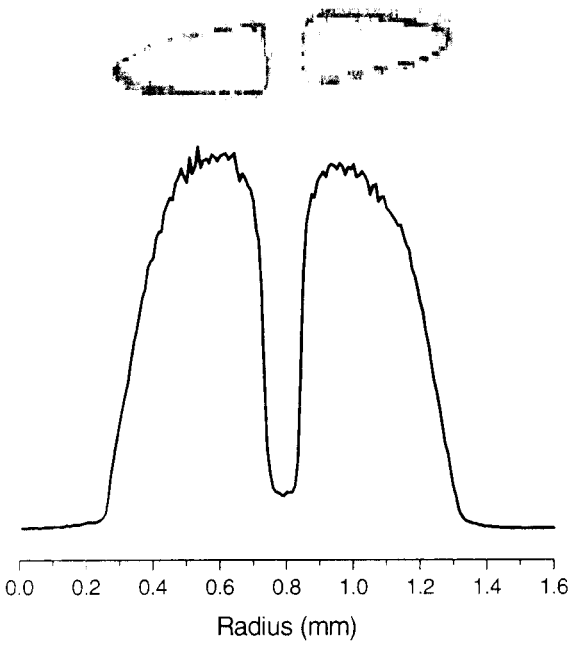

Fig. 3. Two-species $^9Be^+$–e^+ plasma: (top) camera image and (bottom) radial variation of fluorescence signal integrated over z.

little change in the volume of the central dark region was observed after the ^{22}Na source was blocked for 12 h. This indicates that most of the dark central region in Fig. 3 is due to positrons rather than impurity ions of light mass.

3.3. Positron annihilation

To further verify that the dark central column in Fig. 3 is due to accumulated positrons, we pulsed the e^+–$^9Be^+$ plasma onto the 7 μm Ti foil located above the trap and detected the resulting positron annihilation radiation. With the energy (<1 keV) that the positrons acquire during the pulse, all of the positrons annihilate in the Ti foil. The positron annihilation radiation was detected with a NaI scintillation crystal mounted 2.5 or 5 cm above the Ti foil. A light pipe coupled the output of the NaI crystal to a photomultiplier tube mounted a few feet above the magnet. (The ^{22}Na source is removed from the magnet bore during this procedure.) In addition to detecting positrons that are cooled and centrifugally separated from the laser cooled $^9Be^+$ ions, this method is also sensitive to positrons that may be trapped but not cooled to a point where they centrifugally separate from the $^9Be^+$.

We attempted to eject all the positrons rapidly compared to the rise-time of the NaI crystal scintillation (~300 ns). In this way the scintillation crystal will produce a single pulse, free from background radiation, whose height is proportional to the number of annihilated positrons. Positrons were pulsed with different sets of voltages on the trap electrodes and with different pulse voltages. For example, starting with the e^+–$^9Be^+$ plasma trapped with axially symmetric voltages on the experimental trap, the experimental and load trap voltages were adiabatically changed so that the e^+–$^9Be^+$ plasma was moved to the region of the lower endcap of the load trap, where it was confined by the following electrode potentials: 900, 900, 900, 850, 800, 0, 250 and 100 V. Here the potentials are listed starting with the lower endcap of the experimental trap and moving up. The lower endcap of the load trap was then pulsed from 0 to 500 V by a voltage pulser with a ~50 ns rise-time. The resulting output pulse of the photomultiplier preamplifier was recorded on a digital scope.

For a fixed procedure for positron ejection, the voltage peak of the output pulse was proportional to the amount of light-mass charge measured from side-view images such as Fig. 3. However, changing the electrode potentials and pulse voltages of this procedure produced, in many cases, a different proportionality constant. For some conditions the output annihilation pulse was significantly longer than the scintillator single-event pulse and delayed beyond the scintillator and high-voltage pulse rise-times. This indicated that for these conditions not all the positrons were dumped simultaneously. We believe the reason for this is pick-up and ringing induced by the high-voltage pulse on different trap electrodes. While we could not detect ringing and pick-up sufficient to cause this problem, we could monitor the trap potentials only outside the vacuum system. Therefore, to estimate the number of trapped positrons, only annihilation procedures that produced single-event pulses were used.

The NaI crystal detection system was calibrated with a ~37 kBq (1 μC) ^{68}Ge source. This is a good source for calibration purposes because it is principally a positron emitter (511 keV γ-rays) and relatively free from other major photon emissions. One of the larger uncertainties in the calibration is due to the difference in the size of the ^{68}Ge 511 keV γ-ray source ($\leqslant 5$ mm radius) and the annihilation spot on the Ti foil (<1 mm). Overall we estimate the uncertainty in determining the number of annihilated positrons from the peak of the preamplifier output pulse to be ~25%.

Fig. 4 summarizes the results of a number of positron annihilations done with several different experimental procedures. As discussed above, only annihilation procedures which produced single-event pulses are plotted. Even with this requirement some systematic variation between the different procedures is observed. While we do not understand this variation, the positron number determined by the annihilation method should provide a lower limit for the number of trapped positrons. In all cases the positron number measured by annihilation is greater than the number calculated from the volume of the "dark" column.

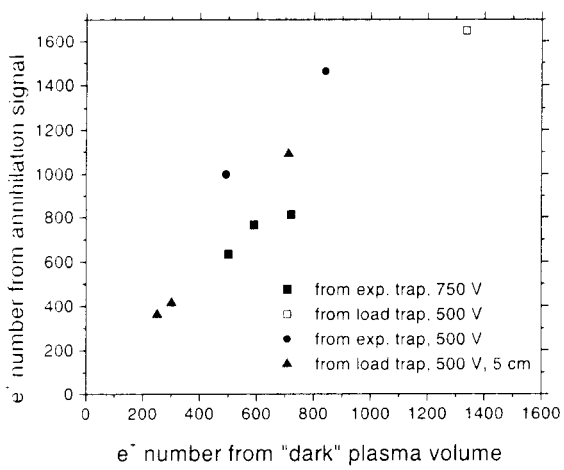

Fig. 4. Comparison of the number of trapped positrons obtained from the calibrated annihilation signal with the number obtained from the volume of the "dark" plasma column. Measurements were taken with the positrons ejected from different traps, with different voltage pulse heights (500–750 V), and with the NaI crystal located 2.5 cm (□, ■ and ●) and 5 cm (▲) from the Ti foil.

However, the ~40% difference is on the order of the combined uncertainty of these two positron measurement methods. Therefore we cannot determine with any certainty whether the number of trapped positrons is greater than indicated by the volume of the "dark" column. However the annihilation measurements do support our claim that most of the light-mass charges in images such as Fig. 3 are positrons that have centrifugally separated from the Be^+ ions.

Centrifugal separation implies that the positrons are rotating with the same rotation frequency as the Be^+ ions and are cold enough to have approximately the same density. We observed centrifugal separation of the positrons with rotation frequencies up to 1 MHz. For larger rotation frequencies, the radius of the positron column was too small to clearly see separation. In the 6 T magnetic field of this experiment $\omega_r \approx 2\pi \times 1$ MHz gives positron densities $\geqslant 4 \times 10^9$ cm^{-3}. This is ~50 times greater than the highest positron density previously achieved [20].

4. Positron accumulation and lifetime

Because of this method's simplicity, we initially attempted to load positrons by following, as much as possible, the method described in [17] of field-ionizing high-Rydberg positronium. We summarize here the accumulation rate obtained with this method. We also plan to accumulate positrons by the method outlined in [2], where positrons are loaded through Coulomb collisions with trapped $^9Be^+$ ions. Results of this method will be discussed in a future publication.

The basic idea from Gabrielse's group is that in high magnetic field a fraction of the moderated positrons that leave the moderator crystal combine with an electron to form positronium in a very high Rydberg state at the moderator crystal's surface. After leaving the crystal, the positronium travels into the trap as long as the electric fields between the moderator and trap are not large enough to field-ionize the Rydberg state. The trap potentials are adjusted to give a larger electric field inside the trap capable of field-ionizing the positronium and therefore capturing the positron. We

accumulated positrons with roughly the same trap potential shape but with different overall well depths (or electric field strengths) than in [17]. Fig. 5 shows one of the smallest trap potentials and the resulting electric field used to accumulate positrons by this method in our setup.

During accumulation, $^9Be^+$ ions were stored in the trap but were at low density because the laser-cooling and rotating wall were turned off. Similar to [17], we were able to accumulate positrons with a reverse bias of a few volts on the moderator crystal which would prevent low-energy positrons from entering the trap. Fig. 6 shows the accumulation of positrons for two different trap depths. The solid curves are fits to the rate equation $dN/dt = a - (N/\tau)$ for the number of accumulated positrons N. Here a is the accumulation rate and $\tau = 200$ h is the positron lifetime obtained from the fit to the lifetime data of Fig. 7. Similar to [17], we observe an increase in the number of accumulated positrons as the maximum electric-field strength within the trap is increased. However, our maximum accumulation rate (trap voltage

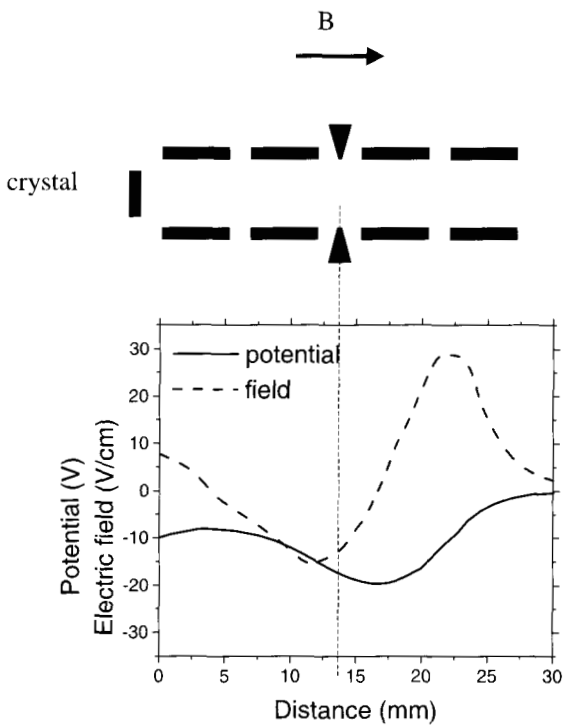

Fig. 5. Schematic diagram of the experimental Penning trap and the on-axis potential well and electric fields used for trapping positrons. This was one of the smaller well depths used to accumulate positrons.

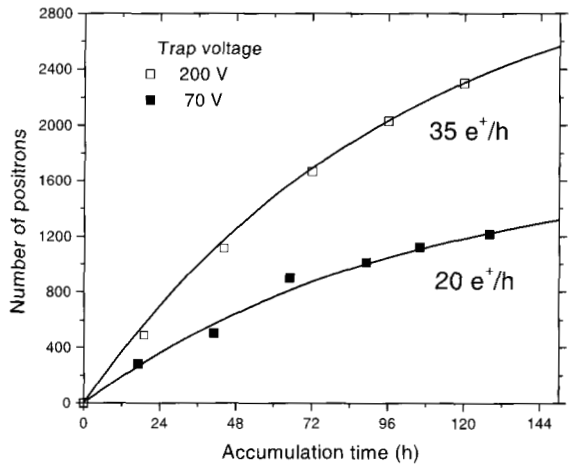

Fig. 6. Number of positrons versus accumulation time for two different trap depths. The 200 V trap corresponds to −40, −38, −200, −220, −200, 0 V and the 70 V trap to −15, −13, −70, −77, −70, 0 V on the moderator crystal and experimental trap electrodes. Here the potential of the moderator crystal is listed first, followed by the experimental trap electrode potentials in order of their proximity to the moderator crystal.

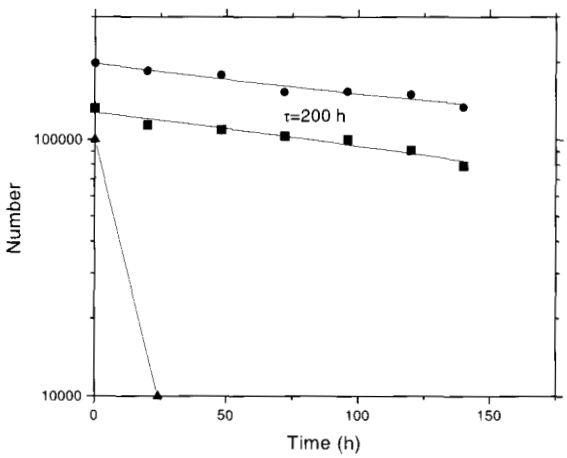

Fig. 7. Lifetime of positrons (●, number shown = actual number × 100), $^9Be^+$ ions (■) and light impurity ions (▲).

~200 V) occurs at an electric-field strength that is 5–10 times greater than observed in [17].

With this method we were able to accumulate a few thousand positrons. However, our accumulation rate was approximately three orders of magnitude lower than that obtained in [16,17] and limited the total number of positrons loaded into the trap. While both experiments were performed in a high magnetic field (5.3 T in [17] and 6 T in our setup), there were substantial differences in the two setups. In particular, [17] used tungsten moderator crystals at cryogenic (4 K) temperatures, compared with the room-temperature Cu moderator used here. They observed that their accumulation rate depended sensitively on the gas absorbed on the surface of the moderator crystal. Heating the moderator while the rest of the trap is at 4.2 K significantly reduced the accumulation rate. Cycling the apparatus to 300 K and back to 4 K restored the accumulation rate. Our Cu moderator crystal was baked with the rest of the trap at 350 °C for about 2 weeks, which may have desorbed much of the adsorbed gases.

Fig. 7 shows the measured lifetime of the positrons, $^{9}Be^{+}$ ions, and light-mass impurity ions. The $^{9}Be^{+}$ ion and positron lifetimes were measured simultaneously on the same plasma by first accumulating positrons and then blocking the ^{22}Na source and measuring the number of $^{9}Be^{+}$ ions and positrons that remained after each day for a week. The trap voltage during the lifetime measurement was −40 V. When the ion and positron numbers were not being measured, the laser-cooling and rotating wall were turned off. The measured lifetime of the positrons was 8 days and is nearly identical to the measured $^{9}Be^{+}$ lifetime. This indicates that the measured positron lifetime could be limited by the trapping lifetime of charged particles in our trap, rather than by annihilation with background gas. We measure the background pressure in our trap to be between 10^{-9} and 10^{-8} Pa. The trap was baked at 350 °C for about 2 weeks and was pumped by a sputter-ion pump and a titanium sublimation pump. For comparison we also show the measured lifetime of light-mass impurity ions. These ions such as H_2^+, H_3^+ or He^+ disappear relatively quickly due to reactions with background gas molecules.

5. Positron temperature estimate

Centrifugal separation of two-species ion plasmas has been observed and studied in $^{9}Be^{+}$–Hg^{+} [31], $^{9}Be^{+}$–$^{26}Mg^{+}$ [33], $^{9}Be^{+}$–Cd^{+} [34] and $^{9}Be^{+}$–$^{136}Xe^{q+}$ ($32 \leqslant q \leqslant 44$) [35] plasmas. In these experiments, laser-cooling of one ion species resulted in temperatures of less than ~1 K for the other ion species. However, the energy transfer in a e^{+}–$^{9}Be^{+}$ collision is ~1000 times weaker than in these previous sympathetic-cooling studies, and therefore it is not reasonable to extrapolate these results to this work. Because we could not find a more direct method, we used the centrifugal separation of the $^{9}Be^{+}$ ions and positrons discussed in Section 3.2 to place an upper limit of about 5 K on the positron temperature of motion parallel to the magnetic field.

For the positron sympathetic-cooling study discussed here we did not measure the $^{9}Be^{+}$ temperature. Previous studies of cooling with a single laser beam directed perpendicularly to the magnetic field and through the plasma center obtained temperatures as low as $T_{\perp} \sim 10$ mK and about five times larger for $T_{\parallel}$ [21–23]. The 11° angle between the laser and the x–y plane in this experimental setup can help lower $T_{\parallel}$. We therefore anticipated $^{9}Be^{+}$ temperatures $\leqslant 100$ mK.

In the 6 T magnetic field of the trap, the positron cyclotron motion is coupled to the room temperature walls (electrodes) of the trap with a ~100 ms time constant. In addition the positron cyclotron motion is collisionally coupled to the positron axial motion, but this coupling becomes exponentially weak when the Larmor radius is less than the distance of closest approach (the strongly magnetized regime). This energy transfer rate has been carefully studied [30] both theoretically and experimentally, and for a 10^{9} cm^{-3} positron plasma is ~10 Hz for $T \sim 10$ K. Therefore we anticipate $T_{\perp}$ to be ~10 K and greater than $T_{\parallel}$, which is reduced by Coulomb collisions with the laser-cooled $^{9}Be^{+}$ ions.

Centrifugal separation has been discussed theoretically by O'Neil [32]. In this case the different charged species were assumed to have the same temperature as required in a global thermal equilibrium state. However, because of the weak ther-

mal coupling between the positrons and $^9Be^+$ ions, the positrons could have a greater temperature than the $^9Be^+$ ions. For example, in the sympathetic cooling study of $^9Be^+$–Hg^+ [31] the Hg^+ ion temperature was 5 to 10 times larger than that of the directly laser-cooled $^9Be^+$ ions. Even with zero temperature $^9Be^+$ ions, the centrifugal separation of the positrons will become less distinct as the positron temperature increases. In order to estimate the effect of the positron temperature on the centrifugal separation we calculated the positron and $^9Be^+$ radial density profiles for an infinitely long column assuming rigid rotation of the plasma but different temperatures. The $^9Be^+$ ions were assumed to be cold ($T_{Be^+} = 0$) and the positron temperature non-zero ($T_{e^+} > 0$). The calculation closely follows the profile calculations discussed in [32,36] and will be discussed more fully in a future publication. Fig. 8(a) shows the results of these calculations for conditions similar to some of the experimental measurements ($\omega_r = 2\pi \times 500$ kHz, positrons/length $= 1.5 \times 10^5$ cm^{-1}). For a given positron temperature, the $^9Be^+$ density makes a sharp jump from zero density at a particular radius. This jump is then followed by a gradual increase at larger radii. As the positron temperature increases, the sharp jump becomes smaller and the subsequent increase in the $^9Be^+$ density more gradual.

We compare these calculations with the experimental profiles shown in Fig. 8(b). In the experimental measurements the plasmas have an axial extent that is typically smaller than the overall plasma diameter (see Fig. 3). However, the calculations, which are for an infinitely long column, should describe the separation of the species as long as the diameter of the dark region in the $^9Be^+$ fluorescence is smaller than the axial extent of the plasma. We typically worked in this regime. Comparison of the profiles in Fig. 8(a) and (b) shows a measured separation that is significantly sharper than that calculated at 10 K and reasonably consistent with the 5 K separation. Also shown in Fig. 8(b) is the measured separation between $^9Be^+$ ions and light-mass ions for the same inner column size. From previous studies of sympathetic cooling [31,33–35] we expect the temperature of both species to be less than 1 K. However,

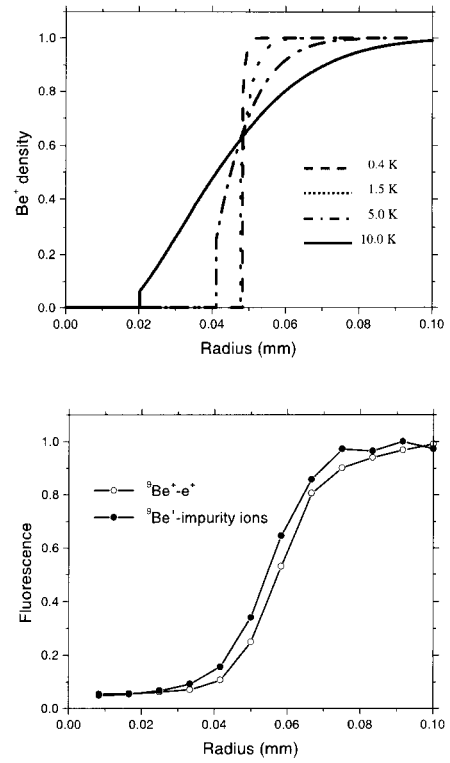

Fig. 8. (a) Calculated radial variation of the $^9Be^+$ ion density for different positron temperatures and (b) measured radial dependence of the fluorescence of scattered laser light for $^9Be^+$–impurity ions and for $^9Be^+$–e^+ plasmas.

because the sharpness of the separation is much worse than calculated for $T = 1$ K, we believe the profile measurements in Fig. 8(b) are limited by the resolution of the imaging-system optics.

We emphasize that this temperature limit is only for positron motion parallel to the magnetic field. For a strongly magnetized plasma the perpendicular kinetic energy is constrained by a many-particle adiabatic invariant [30]. This modifies the particle distribution function with the result that the Debye length is determined by $T_\parallel$ not $T_\perp$ [37].

6. Summary

We have demonstrated sympathetic cooling of positrons by laser-cooled $^9Be^+$ ions. We observed centrifugal separation of the positrons and the

$^9Be^+$ ions, and are able to use this observation to place an upper limit on the positron temperature for motion parallel to the magnetic field of approximately 5 K. The positron perpendicular temperature presumably did not cool below 10 K because the perpendicular and parallel motions decouple for lower temperatures. The observed centrifugal separation implies that the positrons and $^9Be^+$ ions rotate rigidly and have comparable densities, indicating positron densities of $\sim 4 \times 10^9$ cm^{-3}. This is $\sim$50 times greater than the highest positron density previously achieved [20] and could be useful in experiments attempting to make anti-hydrogen. The positron lifetime is greater than 8 days in our room-temperature trap.

The low accumulation rate limited the number of positrons that could be accumulated to a few thousand. This number needs to be significantly increased for most of the potential applications of cold positrons, such as a source for cold beams. This could be done by combining the sympathetic-cooling technique with an established technique for accumulating positrons [15–20]. It is interesting to speculate about the maximum number of positrons that can be sympathetically cooled. A potential limit is the number of ions that can be directly laser-cooled. We can routinely load and laser-cool $\sim 10^6$ $^9Be^+$ ions to temperatures $\leqslant 10$ mK. This ion number is limited by our loading technique rather than by the capabilities of laser-cooling. With a different loading technique non-neutral plasmas of $\sim 10^9$ Mg^+ ions have been laser-cooled to $\sim$1 K temperatures [38]. Therefore $\sim 10^9$ positrons, comparable to the current largest number of trapped positrons, could possibly be sympathetically laser-cooled in a Penning trap. This would provide a useful, very cold source of positrons in a room-temperature vacuum system.

Acknowledgements

Support for this research was provided by the Office of Naval Research. The authors wish to thank Brian Zimmerman and Bert Coursey at the NIST Ionizing Radiation Division for calibrating the activity of the ^{68}Ge source, and Robert Ristenen and Jeffrey Brack for discussion on detecting positron annihilation γ-rays. We thank David Wineland for suggestions through out the experiment and for comments on the manuscript. We also thank Nada Djurić and Jason Kriesel for their comments on the manuscript.

References

[1] D. Wineland, C. Weimer, J. Bollinger, Hyperfine Interac. 76 (1993) 115.
[2] A. Newbury, B.M. Jelenković, J. Bollinger, D. Wineland, Phys. Rev. A 62 (2000) 023405.
[3] R.G. Greaves, C.M. Surko, Phys. Plasmas 4 (1997) 1528.
[4] A. Mills, Hyperfine Interact. 44 (1988) 107.
[5] S. Gilbert, C. Kurtz, R. Greaves, C. Surko, Appl. Phys. Lett. 70 (1997) 1944.
[6] R. Greaves, C. Surko, in: J. Bollinger, R. Spencer, R. Davidson (Eds.), Non-neutral Plasma Physics III, AIP, New York, 1999, p. 19.
[7] J. Bollinger et al., in: E. Ottewitte, W. Kells (Eds.), Intense Positron Beams, World Scientific, Singapore, 1988, p. 63.
[8] J. Malmberg, T. O'Neil, Phys. Rev. Lett. 39 (1977) 1333.
[9] G. Gabrielse, S. Rolston, L. Haarsma, W. Kells, Phys. Lett. A 129 (1988) 38.
[10] M. Glinsky, T. O'Neil, Phys. Fluids B 3 (1991) 1279.
[11] G. Gabrielse, ATRAP Collaboration, Phys. Lett. B 507 (2001) 1.
[12] P. Schwinberg, R.V. Dyck, H. Dehmelt, Phys. Lett. 81 (1981) 119.
[13] R. Conti, B. Ghaffari, T. Steiger, Nucl. Instr. and Meth. A 299 (1990) 420.
[14] H. Boehmer, M. Adams, N. Rynn, Phys. Plasmas 2 (1995) 4369.
[15] L. Haarsma, K. Abdullah, G. Gabrielse, Phys. Rev. Lett. 75 (1995) 806.
[16] G. Gabrielse et al., in: J. Bollinger, R. Spencer, R. Davidson (Eds.), Non-neutral Plasma Physics III, AIP, New York, 1999, p. 29.
[17] J. Estrada et al., Phys. Rev. Lett. 84 (2000) 859.
[18] T. Murphy, C. Surko, Phys. Rev. A 46 (1992) 5696.
[19] C. Surko, S. Gilbert, R. Greaves, in: J. Bollinger, R. Spencer, R. Davidson (Eds.), Non-neutral Plasma Physics III, AIP, New York, 1999, p. 3.
[20] R. Greaves, C. Surko, Phys. Rev. Lett. 85 (2000) 1883.
[21] J. Bollinger, D. Wineland, Phys. Rev. Lett. 53 (1984) 348.
[22] L. Brewer et al., Phy. Rev. A 38 (1988) 859.
[23] W. Itano, L. Brewer, D. Larson, D. Wineland, Phys. Rev. A 38 (1988) 5698.
[24] D. Heinzen et al., Phys. Rev. Lett. 66 (1991) 2080.
[25] X.-P. Huang, J. Bollinger, T. Mitchel, W.M. Itano, Phys. Rev. Lett. 80 (1998) 73.
[26] X.-P. Huang et al., Phys. Plasmas 5 (1998) 1656.
[27] C.A. Murray, A.P. Mills Jr., Solid State Commun. 34 (1980) 789.
[28] R. Wilson, Phys. Rev. B 27 (1983) 6974.

[29] B. Jelenković et al., in: C.M. Surko, F. Gianturco (Eds.), New Directions in Antimatter Chemistry and Physics, Kluwer Academic Publishers, Dordrecht, The Netherlands, 2001, p. 1.
[30] M.E. Glinsky, T.M. O'Neil, M.N. Rosenbluth, Phys. Fluids B 4 (1992) 1156.
[31] J. Larson, J. Bergquist, W. Itano, D. Wineland, Phys. Rev. Lett. 57 (1986) 70.
[32] T.M. O'Neil, Phys. Fluids 24 (1981) 1447.
[33] J. Bollinger et al., IEEE Trans. Instr. Meas. 40 (1991) 126.
[34] H. Imajo et al., Phys. Rev. A 55 (1997) 1276.
[35] L. Gruber et al., Phys. Rev. Lett. 86 (2001) 636.
[36] D.H.E. Dunin, T.M. O'Neil, Rev. Mod. Phys. 71 (1999) 87.
[37] D.H.E. Dunin, T.M. O'Neil, Phys. Rev. Lett. 60 (1988) 511.
[38] E. Holland, F. Anderegg, C. Driscoll, Phys. Rev. Lett. 82 (1999) 4839.